Mice transgenically overexpressing sulfonylurea receptor 1 in forebrain resist seizure induction and excitotoxic neuron death

Catalina Hernández-Sánchez*, Anthony S. Basile†, Irina Fedorova†, Hiroshi Arima‡, Bethel Stannard*, Ana M. Fernandez*, Yutaka Ito*, and Derek LeRoith*§

*Section on Molecular and Cellular Physiology, Clinical Endocrinology Branch, †Laboratory of Bioorganic Chemistry, National Institute of Diabetes and Digestive and Kidney Diseases, and ‡Section on Endocrine Physiology, Developmental Endocrinology Branch, National Institute of Child Health and Human Development, National Institutes of Health, Bethesda, MD 20892

Communicated by John W. Daly, National Institutes of Health, Bethesda, MD, January 4, 2001 (received for review August 28, 2000)

The ability of the sulfonylurea receptor (SUR) 1 to suppress seizures and excitotoxic neuron damage was assessed in mice transgenically overexpressing this receptor. Fertilized eggs from FVB mice were injected with a construct containing SUR cDNA and a calcium-calmodulin kinase IIα promoter. The resulting mice showed normal gross anatomy, brain morphology and histology, and locomotor and cognitive behavior. However, they overexpressed the SUR1 transgene, yielding a 9- to 12-fold increase in the density of [^{3}H]glibenclamide binding to the cortex, hippocampus, and striatum. These mice resisted kainic acid-induced seizures, showing a 36% decrease in average maximum seizure intensity and a 75% survival rate at a dose that killed 53% of the wild-type mice. Kainic acid-treated transgenic mice showed no significant loss of hippocampal pyramidal neurons or expression of heat shock protein 70, whereas wild-type mice lost 68–79% of pyramidal neurons in the CA1–3 subfields and expressed high levels of heat shock protein 70 after kainate administration. These results indicate that the transgenic overexpression of SUR1 alone in forebrain structures significantly protects mice from seizures and neuronal damage without interfering with locomotor or cognitive function.

ATP-sensitive potassium (K_{ATP}) channels are found in cardiac muscle (1) and other excitable cells, including pancreatic β cells, pituicytes, and skeletal and smooth muscle (2). Subcloning and characterization of the molecular components of the K_{ATP} channels reveals that they consist of an inwardly rectifying K^+ channel (K_{ir} 6.1 or K_{ir} 6.2) (3, 4), which is the pore forming subunit with intrinsic sensitivity to ATP, and a sulfonylurea receptor (SUR) subunit (SUR1, SUR2A/B), which enhances K_{ir} sensitivity to ATP and is itself sensitive to MgADP (5–7). Both subunits associate in a 4:4 stoichiometry to form a functional channel (8). Coexpression studies with SUR and K_{ir}6.x isoforms in heterologous systems result in recombinant K_{ATP} channels with different pharmacological and electrophysiological profiles (9–11). Moreover, the complexity of the K_{ATP} channel family is increasing with the characterization of new splice variants (12).

The presence of the K_{ATP} channels in hippocampus, substantia nigra, striatum, and hypothalamus was indicated by pharmacological and electrophysiological studies (13–16). As in peripheral tissues, K_{ATP} channel function is regulated by the ratio of intracellular ATP and ADP concentrations. These channels open to hyperpolarize neurons in response to a decrease in the ratio of ATP/ADP concentrations, thereby linking the membrane potential of neurons to their metabolic status (2). Recently, overlapping expression of SUR and K_{ir}6.x isoforms were found throughout the brain (17, 18), particularly in the hippocampus, where high levels of SUR1, K_{ir}6.2, and K_{ir}6.1 expression are found (17, 18). Although K_{ATP} channels may help regulate seizure thresholds (19, 20) and sensitivity to metabolic stress of neurons in the hippocampus and other brain regions (21–23), this concept remains controversial (13, 16). While some investigations suggest that the neuroprotective actions of SUR openers in the hippocampus *in vitro* may not be mediated by K_{ATP} channels (24, 25), single-cell reverse transcriptase–PCR studies indicate that the heterogeneous K_{ATP} channel subunit composition in hippocampal neuron subpopulations may explain their differential sensitivity to hypoxia and excitotoxicity

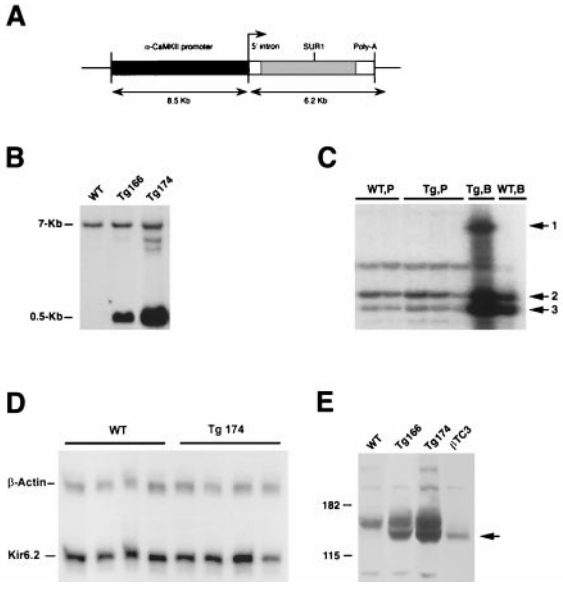

Fig. 1. (*A*) Schematic representation of the CMK-SUR1 construct for production of SUR1 Tg mice. (*B*) Genotyping of Tg mice by Southern blot. Mouse genomic DNA was extracted from mouse tail, digested with *Hin*dIII, and hybridized to a 5′ SUR1 probe. The 7-kb band corresponds to the endogenous mouse SUR1 gene and the 545-bp band corresponds to the transgene. (*C*) An RNase protection assay demonstrates expression of SUR1 transgene in brain (Tg,B, arrow 1), but not in pancreas (Tg,P, arrow 1). Expression of endogenous SUR1 (arrow 3) is roughly equivalent in pancreas (WT,P, $n = 2$; Tg,P, $n = 3$) and brain (WT,B, Tg,B, $n = 1$) from WT and Tg166 mice, relative to β-actin (arrow 2). (*D*) RNase protection assay shows no differences between WT ($n = 4$) and Tg174 ($n = 4$) mice in levels of expression of K_{ir}6.2 message in forebrain. (*E*) SUR1 protein expression in forebrain from WT and Tg174 and Tg166 lines of mice indicated by immunoblot. The positive control consists of 30 μg of protein from a mouse pancreatic β-cell line (βTC3). The arrow points to multiple bands at ≈140 and 150 kDa, consistent with multiple glycosylation states of the SUR1.

Abbreviations: CMK, calcium-calmodulin kinase IIα; Hsp, heat-shock protein; KA, kainic acid; K_{ATP}, ATP-sensitive potassium; K_{ir}, inwardly rectifying potassium; SUR, sulfonylurea receptor; Tg, transgenic; WT, wild type.

§To whom reprint requests should be addressed. E-mail: derek@helix.nih.gov.

The publication costs of this article were defrayed in part by page charge payment. This article must therefore be hereby marked "*advertisement*" in accordance with 18 U.S.C. §1734 solely to indicate this fact.

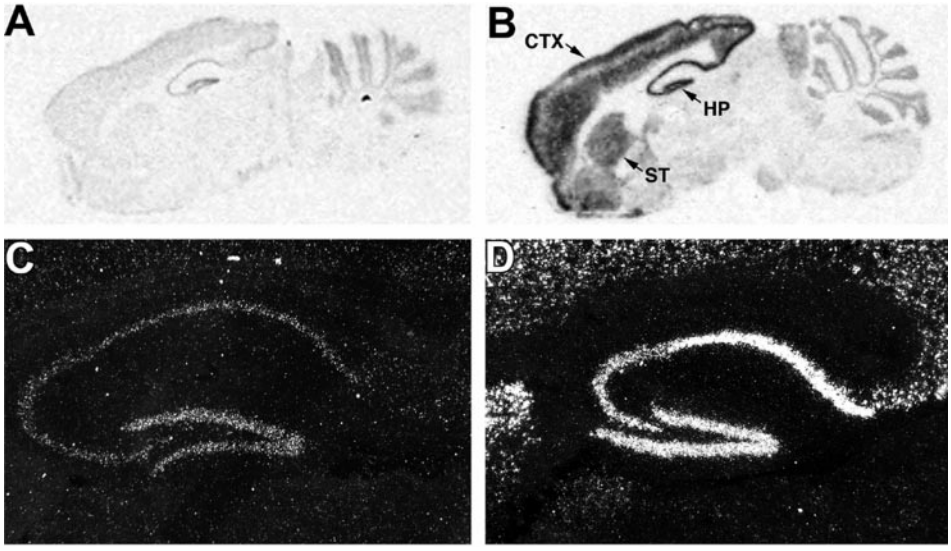

Fig. 2. The SUR1 transgene is specifically expressed in forebrain structures as indicated by *in situ* hybridization. Autoradiographic film exposures of sagittal sections of brain from a WT (*A*) and a Tg174 mouse (*B*) show enhanced message expression in layers II, III, and VI of the cerebral cortex (CTX), striatum (ST), and hippocampus (HP), but not the cerebellum or midbrain structures. Closer examination of the hippocampus using autoradiographic emulsion exposures from a WT (*C*) and a Tg174 mouse (*D*) indicate high levels of expression in the pyramidal neuron layer and dentate gyrus. Magnification: ×50.

(26). Moreover, the inability of SUR openers to penetrate the blood-brain barrier (22) in pharmacologically relevant concentrations prevents studies of the neuroprotective and anticonvulsant properties of these agents from being performed *in vivo*. To gain further insight into the neuroprotective role of K_{ATP} channels in the brain, transgenic (Tg) mice overexpressing the SUR1 subunit in specific forebrain regions were generated by using the calcium-calmodulin kinase II α-subunit (CMK) promoter (27). We now report that the sensitivity of hippocampal pyramidal neurons to kainic acid (KA)-induced hyperexcitability and excitotoxicity was significantly suppressed in Tg mouse lines overexpressing the SUR1 subunit.

Materials and Methods

Molecular Genetics. Hamster SUR1 cDNA was generated by reverse transcriptase–PCR using first-strand cDNA from hamster insulinoma total RNA and oligonucleotides from the hamster SUR1 cDNA sequence (GenBank accession no. L40623)(3). PCR was performed by using *Pfu* DNA polymerase (Stratagene), and the product was sequenced in its entirety to verify fidelity. The pGEM 11-intron cassette vector was generated by subcloning the *Not*I fragment from the pNN265 vector into the *Not*I site of pGEM 11 (Promega). This fragment carries a 230-bp hybrid intron upstream of the *Eco*RV site containing an adenovirus splice donor and Ig splice acceptor (28) and has a simian virus 40 polyadenylation signal downstream of the *Eco*RV site. The hamster cDNA was blunt-ended and subcloned into the *Eco*RV site of the pGEM 11-intron cassette vector, excised with *Not*I along with its flanking regions [5′ hybrid intron and 3′ poly(A) signal], and placed downstream of the 8.5-kb mouse CMK promoter and transcription initiation site. The final ≈15-kb CMK promoter-SUR1 construct was excised by using *Sal*I and *Pst*I (Fig. 1*A*). After checking all cloning junctions by DNA sequencing, the linearized construct was injected into fertilized eggs from FVB/N superovulated female mice. Founder mice were checked for successful integration of the transgene by Southern blot, then backcrossed to FVB/N mice to generate the CMK-SUR1 Tg lines. All mice were maintained in an American Association for the Accreditation of Laboratory Animal Care-certified animal colony, and study protocols were approved by the Animal Care and Use Committee of the National Institute of Diabetes and Digestive and Kidney Diseases, National Institutes of Health.

The hamster SUR1 hybridization probe was generated by subcloning the 552-bp *Hin*dIII fragment from the pGEM 11-intron cassette-hamster SUR1 construct, including the first 428 bp of hamster cDNA, into the *Hin*dIII site of pGEM 3 (Promega). After linearization with *Xho*I, the antisense probe was synthesized by using T7 RNA polymerase with ATP, GTP, [^{35}S]UTP, and [^{35}S]CTP (Amersham Pharmacia) (29).

Blotting and RNase Protection Assays. For Southern blots, mouse tail DNA was prepared, and the DNA fragments were separated on a 0.8% agarose gel, transferred to a nylon membrane, and probed with the mouse 5′ SUR1 probe (18). The 7-kb band corresponds to the endogenous mouse SUR1 gene and the 545-bp band corresponds to the transgene. Western blots of SUR1 protein were performed by using forebrain and midbrain regions. Protein content of supernatant was determined by the BCA assay (Pierce). A sample (100 μg protein) was loaded in reducing buffer onto a 7.5% SDS/PAGE and separated. Resolved proteins were transferred to a nitrocellulose membrane, incubated with anti-SUR1 antibody (1:1,000) (30) and detected with horseradish peroxidase-conjugated anti-rabbit Ig (1:5,000) by using the ECL system (Amersham Pharmacia). The primary antibody was generated against a rat SUR1 peptide corresponding to residues 1569–1581 (CKDSVFASFVRADK).

Western blots of heat-shock protein (Hsp) 70 were performed on hippocampi removed from mice 24 h after KA treatment and homogenized in 0.32 M sucrose. The membrane was incubated with anti-Hsp 70 antibody (StressGen Biotechnologies, Victoria, Canada, 1:1,000), and horseradish peroxidase-conjugated anti-mouse IgG (Amersham Pharmacia, 1:10,000), visualized, then stripped and reblotted by using α-tubulin antibody (Amersham Pharmacia) (1:10,000) and horseradish peroxidase-conjugated anti-mouse IgG (1:10,000). SuperSignal substrate (Pierce) was used for visualization in both cases.

Solution hybridization–RNase protection assays (31) were performed by isolating total RNA from forebrain and pancreas using Trizol reagent (GIBCO/BRL). Brain total RNA (50 μg) was cohybridized with ^{32}P-labeled mouse K_{ir}6.2 (31) and β-actin (Ambion) antisense riboprobes. Pancreatic total RNA (70 μg) was cohybridized with a ^{32}P-labeled mouse antisense SUR1 riboprobe (18) and the hamster SUR1 riboprobe described above.

Histology. Wild-type (WT) and Tg mice were anesthetized with pentobarbital (75 mg/kg), transcardially perfused, and fixed (32). The brains were removed, postfixed, and placed into 20% sucrose/0.025% DMSO overnight, blocked, then flash-frozen in isopentane at −20°C. Serial sections of the entire hippocampus were cut, mounted, stained with 1% cresyl violet, destained, differentiated, and coverslipped.

Table 1. Regional expression of SUR1 message in the brain of WT and SUR1 Tg mice as determined by *in situ* hybridization

Genotype	Frontal cortex, II–III	Frontal cortex, VI	Parietal cortex, II–III	Parietal cortex, VI	Occipital cortex, II–III	Occipital cortex, VI	Caudate	Hippocampal CA1	Hippocampal CA2,3	Dentate gyrus	Cerebellum
WT	0.04 ± 0.00	0.04 ± 0.00	0.04 ± 0.00	0.03 ± 0.02	0.04 ± 0.00	0.04 ± 0.00	0.03 ± 0.00	0.06 ± 0.00	0.05 ± 0.00	0.12 ± 0.01	0.10 ± 0.01
Tg174	0.48 ± 0.03*	0.41 ± 0.02*	0.40 ± 0.02*	0.40 ± 0.02*	0.47 ± 0.03*	0.31 ± 0.03*	0.38 ± 0.03*	0.56 ± 0.01*	0.42 ± 0.02*	0.56 ± 0.01*	0.12 ± 0.01
Tg166	0.23 ± 0.03*	0.20 ± 0.01	0.25 ± 0.02*	0.23 ± 0.01*	0.18 ± 0.02	0.25 ± 0.03*	0.02 ± 0.01	0.36 ± 0.01*	0.30 ± 0.01*	0.43 ± 0.01*	0.11 ± 0.01

Sagittal sections of brain from WT and SUR1 Tg mice from lines 174 and 166 were hybridized with the hamster SUR1 probe, then exposed to film. The calibrated optical density of brain regions in the autoradiographs was measured under ×20 magnification. Each value represents the mean ± SEM of four optical density measures of each brain region from one WT mouse and two mice from each Tg line. *, Significantly different from WT, $P < 0.05$, repeated measures ANOVA followed by Tukey's multiple comparison test.

For *in situ* hybridization, brains were removed, frozen, sectioned, and thaw-mounted onto silanized slides (Fisher Scientific). The sections were postfixed, acetylated, dehydrated, and defatted, then hybridized overnight at 55°C with 2×10^6 cpm of ^{35}S-labeled riboprobe (above, ref. 29). The labeled sections then were dehydrated and exposed to film (Biomax MR, Eastman Kodak) for 4 days, then dipped in film emulsion (Ilford K.5D, Polysciences) and developed after 10 days of exposure.

Morphometric analysis of CA1–3 pyramidal neurons was performed by manually counting neurons in every sixth section of cresyl violet-stained hippocampus at ×400 magnification (32). Area measures of the pyramidal neuron layer (CA1–3) and dentate gyrus of the entire hippocampus were made semiautomatically by digitally acquiring stained regions at ×20 by using shading correction and the same optical density threshold and size filter settings for all sets of mice. Areas then were summed to yield final volume measurements.

Radioligand Binding. Brain regions from WT and Tg mouse lines were removed and disrupted in isotonic Tris-buffered sucrose, pH 7.4 by using a Dounce homogenizer. The homogenates were centrifuged at $1,000 \times g$ (10 min, 0–4°C); the supernatants were retained then centrifuged at $20,000 \times g$ (20 min, 0–4°C). The P2 pellet was reserved, ultrasonically dispersed in 50 mM Tris citrate buffer, centrifuged at $20,000 \times g$, and resuspended in buffer.

The binding assay was performed in duplicate using 50 μl of homogenate, 50 μl [^{3}H]glibenclamide (0.2–6 nM final concentrations, New England Nuclear), and sufficient buffer to yield 500 μl. Nonspecific binding was determined by using 100 μM glibenclamide. The assay was terminated after 90 min of incubation at 25°C by rapid filtration over glass fiber filters. The equilibrium binding constants were determined by using nonlinear regression techniques (PRISM II, GraphPad, San Diego).

Behavioral Studies. Mice were monitored continuously for 2 h after KA administration (25 mg/kg s.c., 0.1 ml) for the onset and extent of seizure activity. Seizures were staged as follows (33): stage 1, immobility; stage 2, forelimb and/or tail extension, rigid posture, and/or running fits; stage 3, repetitive movements, head bobbing; stage 4, rearing and falling; stage 5, continuous rearing and falling; and stage 6, severe tonic-clonic seizures, death. Brains were removed from treated mice after 24 h for immunoblotting or after 5 days for cresyl violet staining.

Mouse locomotor and exploratory behavior was measured in an open field apparatus (Columbus Instruments, Columbus, OH). Mice were habituated to the dimly illuminated test room for 2 h, then placed in the center of the open field. The following behaviors were recorded every 5 min during the 20-min observation period: distance traveled, rearing, time ambulating, time resting, and number of stereotypic movements.

In the first day of passive avoidance studies (pretest), mice were habituated to the apparatus (Columbus Instruments), and the latency to enter the dark avoidance compartment was recorded. Mice failing to enter within criterion time (300 sec) were eliminated. On the second day (acquisition), a mouse was placed in the illuminated start compartment, and the latency to enter the dark chamber was recorded. After entering the dark chamber with all four paws (andiron entry), the door between compartments was closed and a stimulus (0.9 mA, 4 sec) was delivered to the paws. Ten seconds later, the mouse was returned to its home cage. The final (retention) trial was given on the third day using the same protocol, minus the paw stimulus. Latency to enter the dark compartment was recorded, with the maximum time (300 sec) assigned to those mice not re-entering the avoidance chamber.

Results

CMK-SUR1 Tg Mice Overexpress SUR1 Message and Protein in Forebrain. Using a construct containing the CMK promoter linked to the hamster SUR1 cDNA (Fig. 1*A*), seven Tg mouse lines were produced, five of which overexpressed the SUR1 transgene in the forebrain (Fig. 1*B*) relative to WT mice, whereas expression of SUR1 transgene message in peripheral organ systems was not detected (Fig. 1*C*). In addition, the level of $K_{ir}6.2$ message in brain was not increased in Tg relative to WT mice (Fig. 1*D*), as indicated by the ratio of the optical densities of SUR1 or $K_{ir}6.2/\beta$-actin mRNA bands ($K_{ir}6.2$/WT: 170 ± 29 vs. Tg174: 150 ± 58). Immunoblots indicated that SUR1 protein expression was significantly increased in the forebrains of mice from both Tg166 and Tg174 lines (Fig. 1*E*). The proteins in these immunoblot bands have molecular mass of ≈140 and 150 kDa, consistent with previously described differences in glycosylation

Table 2. Equilibrium constants for [^{3}H]glibenclamide binding to brain regions from WT and SUR1 Tg mouse lines

Genotype	Constant	Cortex	Striatum	Hippocampus	Cerebellum
WT ($n = 8$)	K_d, nM	1.2 ± 0.42	1.1 ± 0.17	1.3 ± 0.16	0.9 ± 0.18
	B_{max}, pmol/mg protein	0.37 ± 0.04	0.40 ± 0.08	0.38 ± 0.04	0.34 ± 0.04
Tg174 ($n = 6$)	K_d, nM	1.4 ± 0.16	0.76 ± 0.14	0.69 ± 0.12	0.65 ± 0.11
	B_{max}, pmol/mg protein	5.3 ± 0.71*†	2.2 ± 0.36*	1.8 ± 0.22*	0.78 ± 0.08
Tg166 ($n = 6$)	K_d, nM	1.6 ± 0.36	1.1 ± 0.44	1.1 ± 0.48	0.60 ± 0.09
	B_{max}, pmol/mg protein	2.1 ± 0.36*	1.4 ± 0.17	1.5 ± 0.58	0.52 ± 0.14

[^{3}H]Glibenclamide binding to cell membranes from brain regions dissected from WT and Tg mice was assessed by using saturation assays. Values represent the mean ± SEM. The striata and hippocampi from two mice were pooled for each assay.

*, Significantly different from WT mice, $P < 0.05$, ANOVA followed by Tukey's multiple comparison test.

†, Significantly different from Tg166 mice, $P < 0.05$, ANOVA followed by Tukey's test.

NEUROBIOLOGY

Table 3. Seizure behavior after systemic administration of kainic acid to WT and SUR1 Tg mice

Genotype	Maximum seizure score	Mortality rate
WT	4.6 ± 0.16	17/32
Tg174	2.9 ± 0.43*	4/18†
Tg166	3.7 ± 0.53*	3/11†

Seizures were scored for each mouse for 2 hr after injection with KA (25 mg/kg) with 6 as the highest value. Values represent the mean ± SEM of the maximum seizure intensity recorded for each mouse.

*, Significantly different from WT, $P < 0.05$, ANOVA followed by Tukey's multiple comparison test.

†, Significantly different from WT, $P < 0.05$, Fisher's exact test.

status of SUR1 (34). All Tg mouse lines showed normal growth and body weights and mated normally.

Subsequent analyses of the Tg174 and Tg166 lines showed grossly normal brain morphology and histology. However, *in situ* hybridization (Fig. 2, Table 1) revealed a significant enrichment of SUR1 transgene expression in layers II, III, and VI of the cerebral cortex, the pyramidal neuron layer subfields of the hippocampus, and the caudate from Tg mice relative to WT. There was no significant enrichment of the SUR1 transgene in the cerebellum. Differences in the relative expression of SUR1 transgene (Figs. 1*B* and 2) and protein (Fig. 1*E*) in the different lines led to the characterization of SUR1 density in enriched plasma membrane preparations from different brain regions using radioligand binding techniques (Table 2). No significant differences in the affinity (K_d) of [^{3}H]glibenclamide for SUR were observed regardless of brain region or mouse line investigated. However, SUR density (B_{max}) was significantly elevated above WT levels in a number of forebrain structures, particularly in the cerebral cortex of Tg166 and Tg174 lines and the hippocampus and striatum of Tg174 mice. The density of cerebellar SUR in either Tg line was not significantly different from WT.

Although SUR1 message and protein expression were markedly increased in the forebrain, there were no significant differences between WT and Tg174 mice in any aspect of their locomotor behavior, including: distance traveled in the open field (10,400 ± 470 vs. 10,600 ± 480 cm, WT vs. Tg174, $n = 9$ and 12, respectively); time ambulating (430 ± 19 vs. 420 ± 18 sec); number of stationary movements (570 ± 31 vs. 630 ± 20); or number of vertical movements (1,800 ± 120 vs. 1,900 ± 400). Similarly, the cognitive functions of WT and Tg174 mice as assessed in the passive avoidance test were not significantly different. Not only were the pretest latencies of WT and Tg174 mice similar (69 ± 8.1 vs. 70 ± 10 sec), but the absolute retention times were uniformly high (210 ± 23 vs. 200 ± 29 sec).

CMK-SUR1 Tg Mice Resist KA-Induced Seizures and Neurotoxicity. The CMK-SUR1 Tg174 mice were significantly more resistant to KA-induced seizures than WT mice as assessed by either seizure intensity or mortality rate (Table 3). More than 70% of the Tg174 and Tg166 mice survived for 5 days after KA administration, compared with 46% of WT, and the average maximum intensity of seizures observed in Tg174 mice decreased 36%. Tg166 mice showed a trend toward reduction of KA-induced seizure intensity, but this reduction did not reach significance.

The suppression of seizures and overall survival of Tg174 mice after KA administration is consistent with the preservation of hippocampal pyramidal neurons, which are sensitive to KA-induced excitotoxicity (35). Morphometric analysis of the dentate gyrus and pyramidal neuron layer in cresyl violet-stained sections of hippocampus 5 days after KA treatment (Fig. 3) revealed a marked decrease in stained volume of the pyramidal neuron layer (CA1-CA3) of WT + KA-treated mice (Figs. 3*B* and 4*B*) compared with the control, WT + saline-treated mice. In contrast, there was no significant change in pyramidal neuron layer volume in either Tg174 + KA or Tg166 + KA mouse groups. No change in the volume of the dentate gyrus was observed for any animal group (Figs. 3 *A*, *C*, and *D* and 4*A*).

Although there was no significant loss of pyramidal neuron layer volume in the Tg166 + KA group, a trend toward a decrease was noted. Closer examination revealed that small, intensely stained cells (glia) occupied this layer in place of pyramidal neurons and could be responsible for the measured staining. Manual neuron counts were performed in 2–3 regional samples from the CA1, CA2, and CA3 subfields of the pyramidal neuron layers in every sixth section of hippocampus. Only cells with recognizable nuclei and somatic areas between 200 and 500 μm^2 were counted. As suggested by the volume assessments, the WT + KA mice were extensively lesioned relative to WT + saline controls, with the

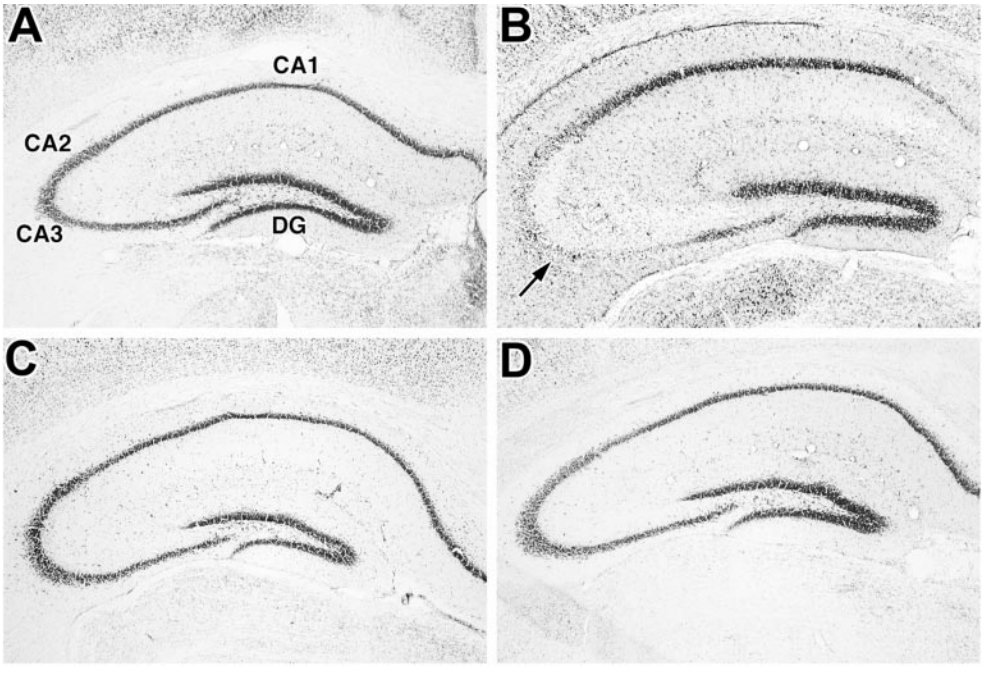

Fig. 3. Comparison of KA-induced damage to pyramidal neurons in the hippocampus of WT (*A* and *B*) and SUR1 Tg174 (*C* and *D*) mice. Coronal sections of hippocampus were cut from WT and SUR1 Tg mouse brains taken 5 days after administration of saline (*A* and *C*) or 25 mg/kg KA (*B* and *D*) and stained with cresyl violet. Note the significant loss of pyramidal neurons in the CA2 and CA3 subfields (arrow) of the KA-treated WT mouse (*B*). No comparable loss of neurons is observed in the KA-treated SUR1 Tg mouse (*D*). Magnification: ×50.

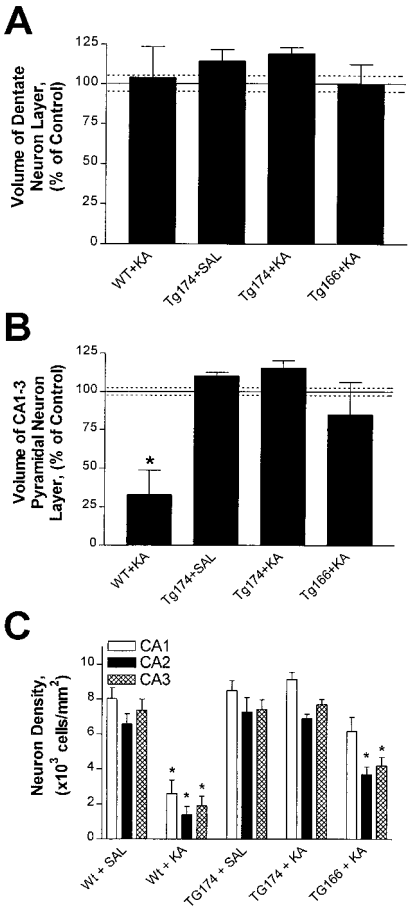

Fig. 4. Hippocampal pyramidal neurons from SUR1 Tg174 mice are resistant to KA-induced excitotoxicity. Reconstruction of the dentate gyrus (*A*) and the pyramidal neuron layer (*B*) of the hippocampus using morphometric analysis of cresyl violet-stained sections of the entire hippocampus allowed the determination and comparison of pyramidal neuron layer volumes. Volume decreased in the pyramidal neuron layer of the WT + KA group (*B*), but no significant decrease in dentate gyrus volume (*A*) was observed after KA administration to any of the mice (WT, TG174, TG166 + KA). Manual counts of pyramidal neurons in the CA1, CA2, and CA3 subfields revealed a significant loss of neurons in the WT + KA group CA1, CA2, and CA3, and the CA2 and CA3 from the TG166 + KA group. However, there was no significant neuronal loss observed in mice from the Tg 174 + KA group. *, Significantly different from control (WT + saline), $P < 0.05$, ANOVA followed by Tukey's multiple comparison test. (*A*), Significantly different from WT + KA group, $P < 0.05$, ANOVA followed by Tukey's multiple comparison test.

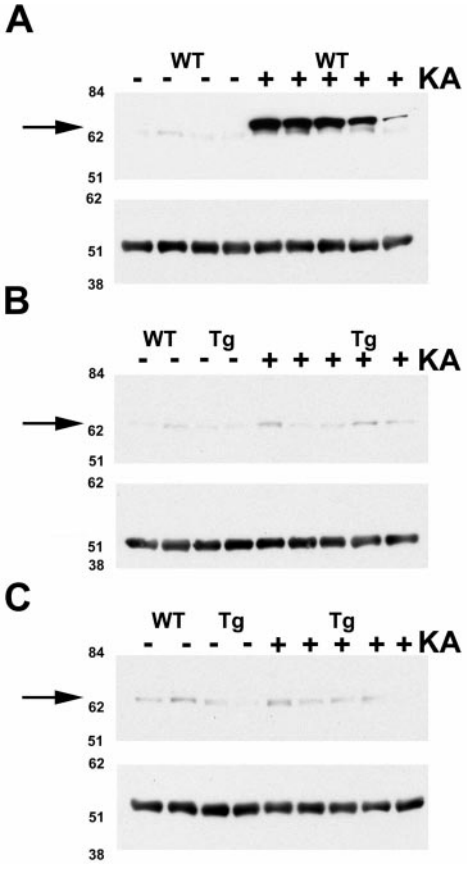

Fig. 5. Immunoblots using anti-Hsp70 antibody indicate that KA administration induces Hsp70 in WT mice (*A*), but not in SUR1 Tg174 (*B*) or Tg166 (*C*) mice. The hippocampus was dissected from WT and SUR1 Tg mice 24 h after injection of 25 mg/kg KA. Each lane contains 30 μg of total hippocampal protein from a single mouse. Molecular weight standard positions are displayed on the left, and arrows indicate the band corresponding to Hsp70. (*A–C Lower*) α-Tubulin bands are shown. Minus and plus signs denote saline- and KA-treated mice, respectively.

number of pyramidal neurons decreased 68%, 74%, and 79% in the CA1, CA2, and CA3 subfields, respectively (Fig. 4*C*). Tg174 + KA mice showed no significant loss of pyramidal neurons, whereas mice in the Tg166 + KA group suffered an intermediate degree of neuron loss (≈44%) in the CA2 and CA3 subfields relative to the WT + KA and Tg174 + KA groups.

An additional biochemical index of KA-induced neuronal damage was hippocampal Hsp70 expression (22, 36, 37). Twenty-four hours after KA treatment, 4/5 WT mice displayed marked induction of hippocampal Hsp70 (Fig. 5*A*, WT +) as indicated by immunoblot. In contrast, Tg174 and Tg166 mice treated with KA showed little or no Hsp70 expression (Fig. 5 *B* and *C*, Tg +). The differences in the level of KA-induced Hsp70 expression do not reflect variances in the total protein loaded as demonstrated by similar levels of α-tubulin in each sample.

Discussion

K_{ATP} channels are expressed in a variety of peripheral tissues and throughout the brain (2). Conditions that reduce the ratio of ATP/ADP concentrations, such as metabolic stress or seizure initiation, stimulate channel opening and lead to neuronal hyperpolarization. However, it is difficult to assess the therapeutic significance of brain K_{ATP} channels in animal models of ischemia, trauma, or seizure disorders because of the inability of pharmacologic modulators of these channels to cross the blood-brain barrier (22, 38).

Recent studies indicate that uncoupled $K_{ir}6.x$ subunits exist in hippocampal pyramidal neurons (17, 26). Tg mice overexpressing SUR1 subunits may have a higher density of functional K_{ATP} channels in the hippocampus and other brain regions, thus reducing their susceptibility to metabolic stress-induced neuronal damage. This hypothesis, and the role of K_{ATP} channels in suppressing seizures and neuronal death, was investigated by generating SUR1 Tg mice, treating them with the excitotoxin KA, and assessing their susceptibility to seizures and neuronal death by using a number of behavioral and neurochemical techniques.

Several Tg mouse lines were created by using hamster SUR1 cDNA. Inserted into the pGEM vector was the SUR1 cDNA, a CMK promoter, an adenovirus splice donor and an Ig splice acceptor, a combination that targets expression of the SUR1 transgene to forebrain regions where the endogenous gene is normally expressed (18), and enhances the probability of transgene expression (28). This vector construct resulted in the successful expression of very high densities of SUR1 protein in

the cerebral cortex (14-fold above WT), with lesser increases (4-fold above WT) in the caudate and hippocampus (Fig. 2, Table 2) without changes in SUR expression in peripheral organs (Fig. 1*C*). Despite the substantial increase in SUR1 expression in brain regions critically involved in motor function, anxiety, or learning and memory processes, neither brain anatomy nor behavior was significantly altered in these mice. These observations are consistent with the lack of effect of the K_{ATP} channel on neurotransmitter release under normoxic conditions (20).

Administering KA to experimental animals induces seizure patterns analogous to human temporal lobe epilepsy (35) by suppressing GABAergic neurotransmission in the hippocampus (39). This leads to hyperexcitability states in pyramidal neurons, ultimately killing those neurons in CA1–3 subfields by excitotoxic mechanisms (40, 41). Further, the FVB mice used as the background strain for the SUR1 Tg mice are highly sensitive to KA-induced seizures (33, 40). Despite this enhanced basal susceptibility, KA-induced seizure intensity and mortality were significantly reduced in Tg174 mice relative to WT. Further, KA-treated Tg174 mice showed little or no loss of hippocampal pyramidal neurons and did not express Hsp70, a marker of seizure severity and neuronal injury (36, 37). A plausible mechanism for this neuroprotection involves the activation of a greater number of functional K_{ATP} channels as a result of the persistent decrease in pyramidal neuron ATP caused by KA-induced hyperexcitation and seizure-induced hypoxia. The magnitude of the resulting potassium current may sufficiently hyperpolarize neurons to compensate for the KA-induced depolarization, thereby preventing massive calcium influx and associated neurotoxicity (42). The incomplete neuroprotection observed in the Tg166 mice, which express a lower density of SUR1, suggests that differences in either the uniformity of expression between individual mice or in the efficiency of SUR1/K_{ir}6.X coupling may exist. Alternatively, there may be a threshold of SUR1 density that must be passed to yield a sufficient number of K_{ATP} channels that can overcome the inherent predisposition of FVB mice to excitotoxic neuron damage and seizures. Thus, the differences in seizure susceptibility of the Tg174 and Tg166 mice are indicative of a dose dependency of SUR1 expression, with varying levels of neuroprotection accompanying varying degrees of SUR1 expression.

Because functional K_{ATP} channels contain both SURX and K_{ir}6.X subunits, with the latter subunit lacking from the construct used to create the CMK-SUR1 Tg mice, the precise mechanism for suppressing KA-induced seizures in these mice remains unclear. Single-cell reverse transcriptase–PCR analysis indicates that only a small subpopulation of CA1 pyramidal neurons express the appropriate combination of subunits to yield functional K_{ATP} channels (26), despite high levels of expression of K_{ir}6.X message throughout the hippocampal pyramidal neuron layer (17). Overexpression of SUR1 in Tg mice may enhance coupling with endogenous K_{ir}6.X subunits, thereby elevating the density of functional K_{ATP} channels capable of hyperpolarizing neurons in response to metabolic stress. This mechanism may protect neurons in other forebrain regions of the CMK-SUR1 Tg mice, such as the basal ganglia and cerebral cortex, where K_{ir}6.X expression surpasses that of SUR1 (17). Alternatively, the presence of exogenous SUR1 may drive the expression of more endogenous K_{ir}6.X to yield neuroprotective densities of functional K_{ATP} channels. Given that K_{ir}6.2 mRNA levels in the Tg174 mice are the same as WT, and that forebrain SUR1 protein expression is dramatically increased in the Tg174 line, exceptional increases in the translation of K_{ir}6.X message would be required to support this hypothesis.

Currently, there are no chemotherapeutic agents specific for the K_{ATP} channel that readily cross the blood-brain barrier. Moreover, interaction of such agents with peripheral organ systems expressing K_{ATP} channels may cause deleterious side effects. Therefore, regionally selective overexpression of a SUR1 transgene by application of appropriate vectors may constitute a novel therapeutic application for the protection of neurons against hyperexcitability and excitotoxicity phenomena. Unlike the use of ionotropic glutamate receptor antagonists to suppress excitotoxic neuron damage, overexpression of the SUR1 subunit has no detectable effect on motor function, cognitive processes, or consciousness. Furthermore, the widespread overexpression of SUR1 in the forebrain of Tg mice in this study suggests that neurons in this area may be protected under other conditions of acute or chronic metabolic stress, such as focal or global ischemia (22). Thus, activation of SUR1 gene expression may represent a mechanism by which "preconditioning" of susceptible central nervous system neuronal populations can be effected at little functional cost (20).

We thank Drs. Mark Mayford (University of California, San Diego) for the CMK promoter and pNN265 plasmids, Jorge Ferrer (Hospital Clinic, Barcelona) for the anti-SUR1 antibody and hamster SUR1 cDNA, Jeffrey Kopp and Huiyan Lu for their assistance in the generation of the CMK-SUR1 Tg mice, and Lisa Heron (National Institutes of Health) for her help with animal handling.

1. Noma, A. (1983) *Nature (London)* **305,** 147–148.
2. Ashcroft, S. J. H. & Ashcroft, F. M. (1990) *Cell. Signalling* **2,** 197–214.
3. Inagaki, N., Gonoi, T., Clemente, J. P., Namba, N., Inazawa, J., Gonzalez, G., Aguilar-Bryan, L., Seino, S. & Bryan, J. (1995) *Science* **270,** 1166–1170.
4. Sakura, H., Ammala, C., Smith, P. A., Gribble, F. M. & Ashcroft, F. M. (1995) *FEBS Lett.* **377,** 338–344.
5. Aguilar-Bryan, L., Nichols, C. G., Wechsler, S. W., Clemente, J. P., Boyd, A. E., Gonzalez, G., Herrera-Sosa, H., Nguy, K., Bryan, J. & Nelson, D. A. (1995) *Science* **268,** 423–426.
6. Chutkow, W. A., Simon, M. C., Le Beau, M. M. & Burant, C. R. (1996) *Diabetes* **45,** 1439–1445.
7. Tucker, S. J., Gribble, F. M., Zhao, C., Trapp, S. & Ashcroft, F. M. (1997) *Nature (London)* **387,** 179–181.
8. Clement, J. P., Kunjilwar, K., Gonzalez, G., Schwanstecher, M., Panten, U., Aguilar-Bryan, L. & Bryan, J. (1997) *Neuron* **18,** 827–838.
9. Inagaki, N., Gonoi, T., Clement, J. P., Wang, C.-Z., Aguilar-Bryan, L., Bryan, K. & Seino, S. (1996) *Neuron* **16,** 1011–1017.
10. Yamada, M., Isomoto, S., Matsumoto, S., Kondo, C., Shindo, T., Horio, Y. & Kurachi, Y. (1997) *J. Physiol. (London)* **499,** 715–720.
11. Okuyama, Y., Yamada, M., Kondo, C., Satoh, E., Isomoto, S., Shindo, T., Horio, Y., Kitakaze, M., Hori, M. & Kurachi, Y. (1998) *Pflügers Arch.* **435,** 595–603.
12. Sakura, H., Trapp, S., Liss, B. & Ashcroft, F. M. (1999) *J. Physiol. (London)* **521,** 337–350.
13. Mourre, C., Ben-Ari, Y., Bernardi, H., Fosset, M. & Lazdunski, M. (1989) *Brain Res.* **486,** 159–164.
14. Ashford, M. L. J., Boden, P. R. & Treherne, J. M. (1990) *Br. J. Pharmacol.* **101,** 531–540.
15. Schwanstecher, C. & Panten, U. (1993) *Arch. Pharmacol.* **348,** 113–117.
16. Lee, K., Dixon, A. K., Freeman, T. C. & Richardson, P. H. (1998) *J. Physiol. (London)* **510,** 441–453.
17. Karschin, C., Ecke, C., Ashcroft, F. M. & Karschin, A. (1997) *FEBS Lett.* **401,** 59–64.
18. Hernández-Sánchez, C., Wood, T. L. & LeRoith, D. (1997) *Endocrinology* **138,** 705–711.
19. Amoroso, S., Schmid-Antomarchi, H., Fosset, M. & Lazdunski, M. (1990) *Science* **247,** 852–854.
20. Plamondon, H., Blondeau, N., Heurteaux, C. & Lazdunski, M. (1999) *J. Cereb. Blood Flow Metab.* **19,** 1296–1308.
21. Ben-Ari, Y., Krnjevic, K. & Crepel, V. (1990) *Neuroscience* **37,** 55–60.
22. Heurteaux, C., Bertaina, V., Widmann, C. & Lazdunski, M. (1993) *Proc. Natl. Acad. Sci. USA* **90,** 9431–9435.
23. Fujimura, N., Tanaka, E., Yamamoto, S., Shigemori, M. & Higashi, H. (1997) *J. Neurophysiol.* **77,** 378–385.
24. Erdemli, G. & Krnjevic, K. (1996) *Eur. J. Pharmacol.* **304,** 37–47.
25. Hyllienmark, L. & Brismar, T. (1996) *J. Physiol. (London)* **496,** 155–164.
26. Zawar, C., Plant, T. D., Schirra, C., Konnerth, A. & Neumcke, B. (1999) *J. Physiol. (London)* **514,** 327–341.
27. Mayford, M., Wang, J., Kandel, E. R. & O'Dell, T. J. (1995) *Cell* **81,** 891–904.
28. Choi, T., Huang, M., Gorman, C. & Jaenisch, R. (1991) *Mol. Cell. Biol.* **11,** 3070–3074.
29. Arima, H. & Aguilera, G. (2000) *J. Neuroendocrinol.* **12,** 833–842.
30. Hernández-Sánchez, C., Ito, Y., Ferrer, J., Reitman, M. & LeRoith, D. (1999) *J. Biol. Chem.* **274,** 18261–18270.
31. Werner, H., Woloschak, M., Adamo, M., Shen-Orr, Z., Roberts, C. T., Jr. & LeRoith, D. (1989) *Proc. Natl. Acad. Sci. USA* **86,** 7451–7455.
32. Kustova, Y., Sung, E.-G., Morse, D., Sei, Y. & Basile, A. S. (1999) *Mol. Chem. Neuropathol.* **35,** 39–59.
33. Schauwecker, P. E. & Steward, O. (1997) *Proc. Natl. Acad. Sci. USA* **94,** 4103–4108.
34. Nelson, D. A., Bryan, J., Wechsler, S., Clement, J. P. & Aquilar-Bryan, L. (1996) *Biochemistry* **35,** 14793–14799.
35. Ben-Ari, Y. (1985) *Neuroscience* **14,** 375–403.
36. Sloviter, R. S. & Lowenstein, D. H. (1992) *J. Neurosci.* **12,** 3004–3009.
37. Zhang, X., Gelowitz, D. L., Lai, C. T., Boulton, A. A. & Yu, P. H. (1997) *Eur. J. Neurosci.* **9,** 760–769.
38. Gandolfo, G., Gottesmann, C., Bidard, J.-N. & Lazdunski, M. (1989) *Eur. J. Pharmacol.* **159,** 329–330.
39. Rodriguez-Moreno, A., Lopez-Garcia, J. C. & Lerma, J. (2000) *Proc. Natl. Acad. Sci. USA* **97,** 1293–1298.
40. Goelz, M. F., Mahler, J., Harry, J., Myers, P., Clark, J., Thigpen, J. E. & Forsythe, D. B. (1998) *Lab. Anim. Sci.* **48,** 34–37.
41. Benedikz, E., Casaccia-Bonnefil, P., Stelzer, A. & Bergold, P. J. (1993) *NeuroReport* **5,** 90–92.
42. Lauritzen, I., De. Weille, J. R. & Lazdunski, M. (1997) *J. Neurochem.* **6,** 1570–15799.